TOPOLOGICAL PHASE TRANSITIONS IV: DYNAMIC THEORY OF BOUNDARY-LAYER SEPARATIONS

Tian Ma, Shouhong Wang

TOPOLOGICAL PHASE TRANSITIONS IV: DYNAMIC THEORY OF BOUNDARY-LAYER SEPARATIONS

TIAN MA AND SHOUHONG WANG

Abstract. We present in this paper a systematic dynamic theory for boundary-layer separations of fluid flows and its applications to large scale ocean circulations, based on the geometric theory of incompressible flows developed by the authors. First, we derive the separation equations, which provide necessary and sufficient conditions for the flow separation at a boundary point. Second, these separation equations are then further converted to predicable conditions, which can be used to determine precisely when, where, and how a boundary-layer separation occurs. Third, we derive conditions for the formation of vortices from boundary tip points, and conditions for the formation of surface turbulence. Fourth, we derive the mechanism of the formation of the subpolar gyre and the formation of the small scale wind-driven vortex oceanic flows, in the north Atlantic ocean.

Contents

Date: December 26, 2017.

Key words and phrases. topological phase transition, dynamic phase transition, boundary-layer separation, Navier-Stokes equations, structural stability, structural bifurcation, separation equation, predicable conditions, vortex formation, boundary tip point, surface turbulence, double gyre ocean circulations, subpolar gyre, subtropical gyre, oceanic vortices.

The work was supported in part by the US National Science Foundation (NSF), the Office of Naval Research (ONR) and by the Chinese National Science Foundation.

1. Introduction

Boundary-layer separation phenomenon is one of the most important processes in fluid flows, and there is a long history of studies which go back to the pioneering work of L. Prandtl [13] in 1904. Basically, in the boundary-layer, the shear flow can detach/separate from the boundary, generating vortices and leading to more complicated turbulent behavior. It is important to characterize the separation.

The aim of this paper is to present a dynamic theory of boundary-layer separations of fluid flows and its applications to large scale ocean circulations. This is part of the research program initiated recently by the authors on the theory and applications of topological phase transitions, including

(1) quantum phase transitions [9],
(2) formation of galactic spiral structure [10],
(3) formation of sunspots and solar eruptions [11], and
(4) interior separation of fluid flows.

As discussed in [9], phase transition is a universal phenomena of Nature. The central problem in statistical physics and in nonlinear sciences is on phase transitions. All phase transitions in Nature that we have encountered can be classified into the following two types:

(1) dynamical phase transitions, and
(2) topological phase transitions (TPTs), also called the pattern formation transitions.

The notion of dynamic phase transition is applicable to all dissipative systems, including nonlinear dissipative systems in statistical physics,

fluid dynamics, atmospheric and oceanic sciences, biological and chemical systems etc. The systematic dynamic transition theory and its various applications are synthesized in [7].

TPTs are entirely different from dynamic phase transitions. Intuitively speaking, a TPT refers to the change of the topological structure in the physical space as certain system control parameter crosses a critical threshold. The notion of TPTs is originated from the pioneering work by J. Michael Kosterlitz and David J. Thouless [2], where they identified a completely new type of phase transitions in two-dimensional systems where topological defects play a crucial role. With this work, they received 2016 Nobel prize in physics.

Both dynamic transitions and TPTs occur in transitions of fluid flows. A topological phase transition and a dynamical phase transition may occur at different critical thresholds. For the example, the formation of the Taylor vortices for the Taylor-Couette-Poiseuille flow studied in [6] is a topological phase transition, which occurs at a different Taylor number than that for the dynamical transition of the problem.

The main ingredients of the paper are as follows.

First, as a TPT study the change in its topological structure in the physical space of the system, the geometric theory of incompressible flows developed by the authors plays a crucial role for the study of TPTs of fluids, including in particular the boundary-layer separation studied in this paper and the interior separation in the forthcoming paper [8]. The complete account of this geometric theory is given in the authors' research monograph [5]. This theory has been directly used to study the transitions of topological structure associated with the quantum phase transitions of BEC, superfluidity and superconductivity [9].

Second, one component of this geometric theory is the necessary and sufficient conditions for structural stability of divergence-free vector fields, recalled in this paper in Theorems 2.3 and 2.5. Another component of the theory crucial for the study in this paper is the theorems on structural bifurcations proved in [1, 4] and recalled in Theorems 2.7 and 2.8. These theorems form the kinematic theory for understanding the topological phase transitions associated with fluid flows.

Third, the most difficult and important aspect of TPTs associated with fluid flows is to make connections between the solutions of the Navier-Stokes equations (NSEs) and their structure in the physical space. The first such connection is the *separation equation* [5, Theorem 5.4.1] for the NSEs with the rigid boundary condition; see also

(4.4) detailed notations:

$$\frac{\partial u_\tau(x,t)}{\partial n} = \frac{\partial \varphi_\tau}{\partial n} + \int_0^t [\nu \nabla \times \Delta u + k\nu \Delta u \cdot \tau + \nabla \times f + k f_\tau] \mathrm{d}t. \tag{1.1}$$

In this paper, we derive the following separation equation for the NSE with the free-slip boundary condition; see (4.12):

$$u_\tau(x,t) = \varphi_\tau(x) + \int_0^t \left[\nu \left(\frac{\partial^2 u_\tau}{\partial \tau^2} + \frac{\partial^2 u_\tau}{\partial n^2} \right) - g_\tau(u) + F_\tau \right] \mathrm{d}t, \tag{1.2}$$

where F and g are the divergence-free parts of the external forcing and the nonlinear term $u \cdot \nabla u$ as defined by (4.10) and (4.11).

The separation equations (1.1) and (1.2) provide a necessary and sufficient condition for the flow separation at a boundary point. In other words, the complete information for boundary-layer separation is encoded in these separation equations, which are therefore crucial for all applications.

Fourth, the separation equations (1.1) and (1.2) link precisely the separation point (x, t), the external forcing and the initial velocity field φ. By exploring the leading order terms of the forcing f and the initial velocity field φ (Taylor expansions), more detailed condition, called predicable condition, are derived in [3, 14] for the Dirichlet boundary condition case, and in Section 5.1 for the free boundary condition case.

The separation equations (1.1) and (1.2), as well as the predicable conditions determine precisely when, where, and how a boundary-layer separation occurs.

Fifth, in view of the separation equation (1.1), we see that increasing the curvature k will lead to boundary layer separation, forming vortices. To demonstrate this idea, we consider vortex separation at a boundary tip point $x_0 \in \partial\Omega$. Let t_0 be the time during a vortex separated from the tip point disappears and a new one appears, and t_0 is called the relaxation time for the tip point separation. Then using the separation equation (1.1), we deduce that the critical curvature where vortices begin to form is given by

$$k_c = \frac{a}{|f_\tau| t_0}. \tag{1.3}$$

Here a is the strength of the initial shear flow φ (injection velocity). Physically, $a = |\nabla \varphi(x_0)|$, which is proportional to the viscosity ν, and the frictional force f_τ is proportional to the smoothness κ of the material surface. Therefore, the critical curvature k_c is

$$k_c = \frac{\alpha \nu}{\kappa t_0}, \tag{1.4}$$

where α is the proportional coefficient.

Formula (1.4) shows that vortices are easier to form if the viscosity of fluid is relatively small, and the surface of the material is rougher (i.e. κ is relatively large). This conforms to the physical reality.

Sixth, using the separation equation, we can also determine the critical velocity threshold u_c so that when $u_0 > u_c$, surface turbulence occurs. For simplicity consider a portion of flat boundary $\Gamma = \{(x_1, 0) \mid 0 < x_1 < L\} \subset \partial\Omega$.

Use u_0 as the control parameter, and take the velocity decay property, which is true for moderate sized L:

$$\varphi_\tau = u_0 - \beta_0 \nu x_1 + \beta_2 x_1^2, \qquad \beta_0 \nu > \beta_2 L, \tag{1.5}$$

where $\beta_1 = \beta_0 \nu,\ \beta_2 > 0$ are two small parameters, depending on the viscosity ν of the fluid and the surface physical property of Γ. The damping force takes the form

$$F_\tau = -\gamma u_0^k \qquad \text{with } k > 1,\ \gamma > 0. \tag{1.6}$$

Then we can show that the critical velocity for generating surface turbulence is

$$u_c = \left[\frac{1}{\gamma} \left(\frac{1}{t_0} + \beta_0 \nu \right) \right]^{1/(k-1)}. \tag{1.7}$$

Seventh, the atmospheric and oceanic flows exhibit recurrent large-scale patterns. These patterns, while evolving irregularly in time, manifest characteristic frequencies across a large range of temporal scales, from intraseasonal through interdecadal. The appropriate modeling and theoretical understanding of such irregular climate patterns remain a challenge.

For the ocean, the basin-scale motion is dominated by wind-driven (horizontal) circulation and thermohaline (vertical) circulation, also called meridional overturning circulation. Their variability, independently and interactively, may play a significant role in climate changes, past and future.

Also, the physics of the separation of western boundary currents is a longstanding problem in physical oceanography. The Gulf Stream in the North Atlantic and Kuroshio in the North Pacific have a fairly similar behavior with separation from the coast occurring at or close to a fixed latitude.

One objective of this paper is to derive the mechanism of the formation of the subpolar gyre, as well as the formation of the small scale vortices of wind-driven oceanic flows, in the north Atlantic ocean.

In particular, for the wind-driven north Atlantic circulations, with careful analysis using the separation equations (1.1) and (1.2), we derive the following conclusions:

(1) *If the mid-latitude seasonal wind strength λ exceeds certain threshold λ_c,vortices near the north Atlantic coast will form. Moreover, the scale (radius) of the vortices is an increasing function of $\lambda - \lambda_c$;*
(2) *The condition for the initial formation of the subpolar gyre is that the curvature k of $\partial\Omega$ at the tip point on the east coast of Canada is sufficiently large, and the combined effect of the convexity of the tangential component of the Gulf stream shear flow and the strength of the tangential friction force is positive; and*
(3) *the vortex separated from the boundary tip point is then amplified and maintained by the wind stress, the strong Gulf stream current and the Coriolis effect, leading to the big subpolar gyre that we observe.*

The paper is organized as follows. The basic geometric theory for incompressible flows is recapitulated in Section 2, followed by the description of the boundary-layer phenomena main problems in Section 3. Section 4 derives basic boundary-separation theory, and introduces in particular the separation equations. Section 5 introduces predicable conditions, and obtain conditions for vortex formation near boundary tip points and conditions for transitions to surface turbulence. Section 6 studies the mechanism of the formation of subpolar and subtropic gyres, as well as the small vortices, for the northern Atlantic ocean.

2. Preliminaries for 2D Incompressible Flows

2.1. **Basic concepts.** The state function describing the fluid motion is the velocity field u. The topological phase transition of a fluid system is defined as the change in its topological structure of the velocity field $u(x, \lambda)$ at a critical parameter λ_c, where λ is the time or other physical control parameters.

Let v be a vector field defined on domain $\Omega \subset \mathbb{R}^n$. For each point $x_0 \in \Omega$, v possesses an orbit $x(t, x_0)$ passing through x_0, which is a solution of the ordinary differential equation with x_0 as its initial value:

$$\frac{\mathrm{d}x}{\mathrm{d}t} = v(x),$$
$$x(0) = x_0.$$

The set of all orbits is called the flow of v. Each vector field has its own flow structure, called the topological structure of v. Therefore, we can introduce the notion of topological equivalence for two vector fields.

Definition 2.1. *Let v_1 and v_2 be two vector fields in Ω. We say that v_1 and v_2 are topologically equivalent if there exists a homeomorphism $\varphi : \Omega \to \Omega$ that takes the orbits of v_1 to the orbits of v_2, preserving orientation.*

The main aim of this paper is to study the structure transitions of 2D incompressible fluid flows represented by velocity fields u, which are the solutions of the fluid dynamical equations. To this end, let $C^r(\Omega, \mathbb{R}^2)$ be the space of all r-th order continuously differentiable 2D vector fields on Ω, and let

$$
\begin{aligned}
D^r(\Omega, \mathbb{R}^2) &= \{v \in C^r(\Omega, \mathbb{R}^2) \mid \mathrm{div} v = 0,\ v_n = 0 \text{ on } \partial\Omega\},\\
B^r(\Omega, \mathbb{R}^2) &= \{v \in D^r(\Omega, \mathbb{R}^2) \mid \frac{\partial v_\tau}{\partial n} = 0 \text{ on } \partial\Omega\},\\
B_0^r(\Omega, \mathbb{R}^2) &= \{v \in D^r(\Omega, \mathbb{R}^2) \mid v = 0 \text{ on } \partial\Omega\},
\end{aligned}
$$

where $v_n = v \cdot n$, $v_\tau = v \cdot \tau$, and n, τ are the unit normal and tangent vectors on $\partial\Omega$. The vector fields in $B^r(\Omega, \mathbb{R}^2)$ satisfy the free-slip boundary condition, and vector fields in $B_0^r(\Omega, \mathbb{R}^2)$ satisfy the rigid boundary condition.

Definition 2.2. *Let X be either $B^r(\Omega, \mathbb{R}^2)$ or $B_0^r(\Omega, \mathbb{R}^2)$. A vector field $v \in X$ is called structurally stable in X, if there exits an open neighborhood $U \subset X$ of v such that for any $v_1 \in U$, v and v_1 are topological equivalent.*

2.2. **Structural stability theorems.** In [5], the authors established the geometric theory for 2D divergence-free vector fields, including the structural stability theorems, the boundary-layer and the interior separation theory. In this section, we recapitulate the two structural stability results respectively for $v \in B^r(\Omega, \mathbb{R}^2)$ and $v \in B_0^r(\Omega, \mathbb{R}^2)$, which lay the needed mathematical foundation for the topological phase transitions of fluid dynamics developed in this paper.

1). *Structural stability in $B^r(\Omega, \mathbb{R}^2)$.* The vector fields $v \in B^r(\Omega, \mathbb{R}^2)$ satisfy the free-slip boundary condition, given by

$$
v_n|_{\partial\Omega} = 0, \qquad \left.\frac{\partial v_\tau}{\partial n}\right|_{\partial\Omega} = 0. \tag{2.1}
$$

A point $p \in \Omega$ is called a non-degenerate zero point(or singular point) of v if $v(p) = 0$, and the Jacobian matrix $Dv(p)$ is non-degenerate. A vector field v is regular if all zero points of v are non-degenerate. For

the vector fields with condition (2.1), we have the following structural stability theorem.

Theorem 2.3 ([5, Theorem 2.1.2]). *Let $\Omega \subset \mathbb{R}^2$ be a bounded domain. A vector field $v \in B^r(\Omega, \mathbb{R}^2)$ $(r \geq 1)$ is structurally stable if and only if*

(1) *v is regular;*
(2) *all interior saddles of v are self-connected; and*
(3) *each boundary saddle is connected to a boundary saddle on the same connected component of the boundary.*

Moreover, all structurally stable vector fields in $B^r(\Omega, \mathbb{R}^2)$ form an open and dense set in $B^r(\Omega, \mathbb{R}^2)$.

2). *Structural stability in $B_0^r(\Omega, \mathbb{R}^2)$.* A vector field $v \in B_0^r(\Omega, \mathbb{R}^2)$ $(r \geq 1)$ satisfies the rigid boundary condition, also called the Dirichlet boundary condition:

$$v|_{\partial\Omega} = 0. \tag{2.2}$$

With condition (2.2), all boundary points are singular in the usual sense. Hence we need to introduce the ∂-regular and the ∂-singular points for $p \in \partial\Omega$.

Definition 2.4. *Let $v \in B_0^r(\Omega, \mathbb{R}^2)$.*

(1) *A point $p \in \partial\Omega$ is called a ∂-regular point of v if*

$$\frac{\partial v_\tau(p)}{\partial n} \neq 0;$$

otherwise, $p \in \partial\Omega$ is called a ∂-singular point;

2) *a ∂-singular point p of v is called non-degenerate if*

$$det \begin{pmatrix} \dfrac{\partial^2 v_\tau(p)}{\partial n \partial \tau} & \dfrac{\partial^2 v_\tau(p)}{\partial n^2} \\ \dfrac{\partial^2 v_n(p)}{\partial n \partial \tau} & \dfrac{\partial^2 v_n(p)}{\partial n^2} \end{pmatrix} \neq 0.$$

and a non-degenerate $\partial-$singular point is also called $\partial-$saddle of v; and

(2) *a vector field $v \in B_0^r(\Omega, \mathbb{R}^2)$ is said $D-$regular, if v is regular in the interior of Ω and all $\partial-$singular points are non-degenerate.*

Let $v \in B_0^r(\Omega, \mathbb{R}^2)$ be $D-$regular, then the number of $\partial-$saddles of v is finite, and there is only one orbit connected to a $\partial-$saddle from the interior. In particular, no orbits are connected to a $\partial-$singular point.

We have the following structural stability theorem for incompressible flows with the Dirichlet boundary condition (2.2).

Theorem 2.5 ([5, Theorem 2.2.9])**.** *Let $\Omega \subset \mathbb{R}^2$ be a bounded domain. Then a vector field $v \in B_0^r(\Omega, \mathbb{R}^2)$ $(r \geq 2)$ is structurally stable if and only if*

(1) *v is $D-$regular;*
(2) *all interior saddles of v are self-connected; and*
(3) *each $\partial-$saddle of v is connected to a $\partial-$saddle on the same connected component of the boundary.*

Moreover, all structurally stable vector fields in $B_0^r(\Omega, \mathbb{R}^2)$ form an open and dense set in $B_0^r(\Omega, \mathbb{R}^2)$.

2.3. **Structural bifurcations on boundary.** Let $t \in [0, T]$ be the time parameter, or an other physical parameter, and u be a family of vector fields with t as parameter:

$$u : [0, T] \to X \qquad \text{for } 0 < T < \infty, \tag{2.3}$$

where X is $B^r(\Omega, \mathbb{R}^2)$ or $B_0^r(\Omega, \mathbb{R}^2)$. Let $C^k([0, T], X)$ be the space of all one-parameter family of vector fields $u(t)$ as in (2.3), where $k \geq 0$ is the order of continuous derivatives of u with respect to t.

Definition 2.6. *Let $u \in C^0([0, T], X)$ be a one-parameter family of vector fields in X. We say that $u(x, t)$ has a structural bifurcation at t_0 $(0 < t_0 < T)$, if for any $t^- < t_0$ and $t_0 < t^+$ with t^- and t^+ sufficiently close to t_0 the vector field $u(\cdot, t^-)$ is not topologically equivalent to $u(\cdot, t^+)$.*

We remark that the structural stability theorems, Theorems 2.3 and 2.5, ensure the rationality of Definition 2.6, i.e. the bifurcation point t_0 is isolated.

In the following we introduce the structural bifurcation theorems on the boundary for vector fields in $B^r(\Omega, \mathbb{R}^2)$ or $B_0^r(\Omega, \mathbb{R}^2)$.

1). *Structural bifurcations for free boundary condition.* Let $u \in C^1([0, T], B^r(\Omega, \mathbb{R}^2))$. Take the first order Taylor expression of $u(x, t)$ at $t_0 \in \partial\Omega$ as

$$\begin{aligned} &u(x, t) = u^0(x) + (t - t_0)u^1(x) + o(|t - t_0|), \\ &u^0(x) = u(x, t_0), \\ &u^1(x) = \frac{\partial u}{\partial t}(x, t_0). \end{aligned} \tag{2.4}$$

For the vector fields u^0 and u^1 in (2.4), we make the following assumption. Let $\overline{x} \in \partial\Omega$ satisfy

$$\begin{aligned} &u^0(\overline{x}) = 0, \text{ and } \overline{x} \text{ is isolated singular point,} \\ &u^1_\tau(\overline{x}) \neq 0, \\ &\text{ind}(u^0, \overline{x}) \neq -\frac{1}{2}. \end{aligned} \tag{2.5}$$

Here $\text{ind}(u^0, \overline{x})$ is the Poincaré index of u^0 at $\overline{x}$, defined by

$$\text{ind}(u^0, \overline{x}) = -\frac{n}{2} \quad (n = 0, 1, 2, \cdots),$$

where n is the number of interior orbits of u^0 connected to $\overline{x}$.

Theorem 2.7 (Structural bifurcation for free boundary condition)**.** *Let $u \in C^1([0,T], B^r(\Omega, \mathbb{R}^2))$ have the Taylor expression* (2.4) *at $t_0 > 0$, and for $\overline{x} \in \partial\Omega$ satisfy condition* (2.5)*. Then $u(x,t)$ has a structural bifurcation at $(\overline{x}, t_0)$.*

2). *Structural bifurcation for rigid boundary condition.* Let $u \in C^1([0,T], B^r_0(\Omega, \mathbb{R}^2))$ have the Taylor expression (2.4). For u^0 and u^1 in (2.4) we assume that

$$\begin{aligned} &\frac{\partial u^0(\overline{x})}{\partial n} = 0 \text{ and } \overline{x} \in \partial\Omega \text{ is an isolated singular point,} \\ &\frac{\partial u^1_\tau(\overline{x})}{\partial n} \neq 0, \\ &\text{ind}\left(\frac{\partial u^0}{\partial n}, \overline{x}\right) \neq -\frac{1}{2}. \end{aligned} \tag{2.6}$$

Theorem 2.8 (Structural bifurcation for rigid boundary condition)**.** *Let $u \in C^1([0,T], B^r_0(\Omega, \mathbb{R}^2))$ have the Taylor expression* (2.4) *and satisfy condition* (2.6)*. Then u has a structural bifurcation at $(\overline{x}, t_0)$.*

3. Phenomena and Problems Related to Boundary-Layer Separations

3.1. **Boundary-layer separation phenomena.** Boundary-layer separation is a universal phenomenon in fluid flows, and says that a shear flow near the boundary generates suddenly vortices from the boundary. More precisely, we say that a velocity field $u(x,t)$ has a boundary-layer separation near $\overline{x} \in \partial\Omega$ at $t_0 > 0$, if $u(x,t)$ is topological equivalent to the structure as shown in Figure 3.1(a) for $t < t_0$, and to the structure as in Figure 3.1(b) for $t > t_0$. Namely, if $t < t_0$ then $u(x,t)$ is topological equivalent to a parallel shear flow, and if $t > t_0$, $u(x,t)$ bifurcates to a vortex from $\overline{x} \in \partial\Omega$.

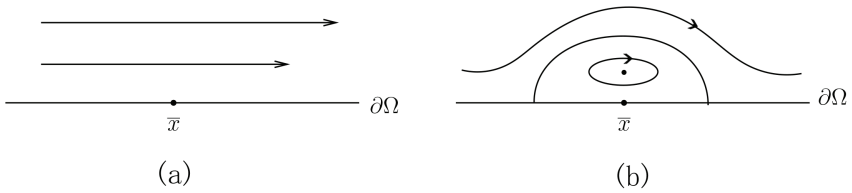

FIGURE 3.1. (a) A parallel shear flow, and (b) a boundary vortex flow.

In the following, we give three remarkable physical phenomena associated with boundary-layer separations.

1). *Formation of surface turbulence.* A surface flow is the fluid motion on a boundary surface, as the parallel shear flows. We know that if the velocity of a surface flow exceeds certain critical value, then the boundary-layer separation will lead to turbulence. During the transition from a parallel shear flow to a surface turbulence, boundary-layer separation must occur. Figure 3.2 provides a schematical diagram to illustrate the the formation process of surface turbulence.

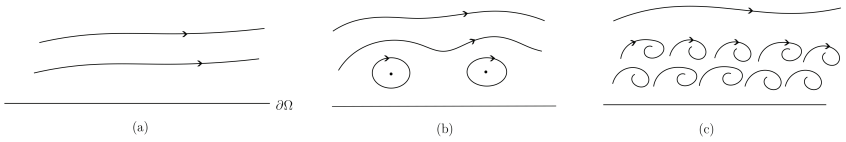

FIGURE 3.2. (a) If the surface velocity $u_0 < u_c$, surface flow is parallel; (b) boundary-layer separation occurs for u_0 near u_c; and (c) if u_0 exceeds u_c, surface turbulence appears.

2). *Vortex flows near a boundary tip point.* At a tip point on the boundary, a fluid flow generates vortices, as shown in Figure 3.3(b); see also [12, Section 4.1.4]. Let $x_0 \in \partial\Omega$ be a tip point with curvature $k(x_0)$. For a given injection velocity u_0, there is a critical curvature k_c such that if $k(x_0) < k_c$, there is no vortices forming near x_0 for the boundary-layer flow shown in Figure 3.3(a), and if $k(x_0) > k_c$ ($k(x_0) = \infty$ at a cusp point), the vortices appear near x_0; see Figure 3.3(b).

3). *Wind-driven Atlantic gyres.* The oceanic gyres are typical large structure of large-scale ocean surface circulations. Figure 3.4 provides the map of the five major oceanic gyres, where the left one is the Indian

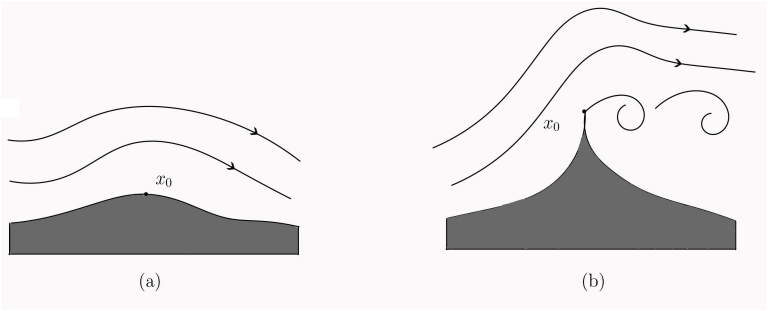

FIGURE 3.3. (a) As the curvature $k(x_0) < k_c$, no vortices near x_0, (b) As $k(x_0) > k_c$, the vortices appear.

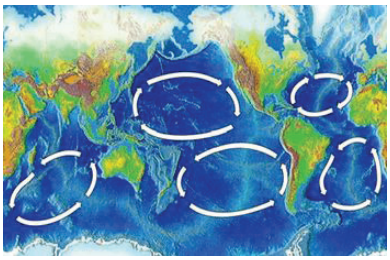

FIGURE 3.4. A global map of major ocean gyres.

ocean gyre, the middle two are the Pacific gyres, and the right two are the Atlantic gyres.

The Atlantic gyres consist of the north Atlantic gyre located in the northern Atlantic and the south Atlantic gyre in the southern Atlantic.

In the northern Atlantic, the trade winds blow westward in the tropics and the westerly winds blow eastward in mid-latitudes. This wind-driven ocean surface flows form a huge and clockwise gyre in the mid-latitude ocean basin, usually called the north Atlantic gyre. In the north of the north Atlantic gyre, there is the north Atlantic subpolar gyre. The mid-latitude gyre and subpolar gyre together are called the north Atlantic double-gyres, which are present permanently; see Figure 3.5(a). Due to the influences of the Gulf Stream and seasonal winds, vortices are separated from the margins of the gyres, and are essentially the phenomena of boundary-layer separation; see Figure 3.5(b).

3.2. **Main problems.** Based on the physical phenomena of boundary-layer separations given above, we now state some basic problems that need to be addressed by the theory of boundary-layer separations.

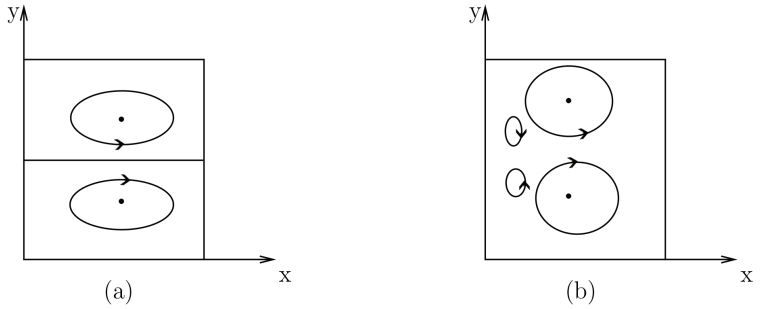

FIGURE 3.5. (a) North Atlantic double-gyres, which are present permanently; (b) vortices separated from the North Atlantic coast.

The boundary-layer separation phenomenon is a typical example of topological phase transitions, and is governed by fluid dynamical equations. Consider the Navier-Stokes equations

$$
\begin{aligned}
&\frac{\partial u}{\partial t} + (u \cdot \nabla)u = \nu \Delta u - \frac{1}{\rho}\nabla p + f, \quad x \in \Omega \subset \mathbb{R}^2, \\
&\mathrm{div} u = 0, \\
&u|_{\partial\Omega} = 0 \qquad \left(\text{or } u_n|_{\partial\Omega} = 0,\ \left.\frac{\partial u_\tau}{\partial n}\right|_{\partial\Omega} = 0 \right), \\
&u(0) = \varphi(x).
\end{aligned} \tag{3.1}
$$

The state function describing boundary-layer separations is the 2D velocity field $u(x, \lambda)$, where λ is the parameter controlling the topological structural transitions of u, and can be taken as the following physical quantities

$$\lambda = t,\ \nu,\ f,\ \varphi,\ k, \tag{3.2}$$

where t is the time, ν is the viscosity, f is the external force, φ is the initial velocity, and k is the curvature of $\partial\Omega$.

The main aspects of a boundary-layer separation theory should include the following:

(1) establish conditions under which the separations occur and determine the critical thresholds;
(2) (predicable problem) develop a theory to determine when, where and how the separation occurs, based on the observable data such as the initial velocity φ, the external force f, and the geometric condition of $\partial\Omega$, etc;
(3) for the surface turbulent phenomena as shown in Figure 3.2, if we take the initial injection velocity u_0 as the control parameter,

then we need to know the critical velocity u_c for the turbulence to occur; and

(4) at the tip point vortices as shown in Figure 3.3(b), provide a relation between the critical curvature k_c, the surface frictional coefficient β of material, and other related physical parameters.

In the remaining part of the paper, we develop a systematic boundary-layer theory, based on the geometric theory of 2D incompressible flows recapitulated in Section 2. The theory we establish solves the problems listed above associated with main components of a boundary-layer theory.

4. Basic Boundary-Layer Theory

4.1. **Boundary-layer separation theorem.** Let $u(x,t)$ be the solution of the Navier-Stokes equations (3.1), and $\Gamma \subset \partial\Omega$ be an open part. For $\overline{x} \in \Gamma$, if there is a time $t_0 > 0$ such that the following conditions hold true:

$$\begin{cases} \begin{cases} \overline{x} \in \Gamma \text{ is an isolated zero of } \dfrac{\partial u_\tau(\cdot,t_0)}{\partial n}, \\ \left.\dfrac{\partial u_\tau}{\partial n}\right|_\Gamma \neq 0 \ \forall\ t < t_0, \\ \dfrac{\partial u_\tau}{\partial n}(\overline{x},t_0) = 0 \end{cases} & \text{for (2.2)}, \\ \begin{cases} \overline{x} \in \Gamma \text{ is an isolated zero of } u_\tau(\cdot,t_0), \\ u_\tau|_\Gamma \neq 0 \ \forall\ t < t_0, \\ u_\tau(\overline{x},t_0) = 0 \end{cases} & \text{for (2.1)}, \end{cases} \tag{4.1}$$

then by the homotopic invariance of the topological index, we have

$$\begin{aligned} &\operatorname{ind}\left(\frac{\partial u(\cdot,t_0)}{\partial n}, \overline{x}\right) = 0 \quad \text{for (2.2)}, \\ &\operatorname{ind}(u(\cdot,t_0), \overline{x}) = 0 \qquad \text{for (2.1)}. \end{aligned} \tag{4.2}$$

We also assume that

$$\begin{aligned} &\frac{\partial}{\partial t}\frac{\partial u_\tau(\overline{x},t_0)}{\partial n} \neq 0 \quad \text{for (2.2)}, \\ &\frac{\partial}{\partial t} u_\tau(\overline{x},t_0) \neq 0 \qquad \text{for (2.1)}. \end{aligned} \tag{4.3}$$

It is clear that conditions (4.1) replaces conditions (4.2). Then by Theorems 2.7 and 2.8, we derive the following boundary-layer separation theorem for the solutions of the Navier-Stokes equations (3.1).

Theorem 4.1 (Boundary-layer separation)**.** *Let $u(x,t)$ be the solution of the Navier-Stokes equations* (3.1)*. If $u(x,t)$ satisfies* (4.1) *and* (4.3)*, then u has a boundary-layer separation at $(\overline{x},t_0)$.*

Remark 4.2. Let $X = B_0^r(\Omega,\mathbb{R}^2)$ or $B^r(\Omega,\mathbb{R}^2)$. Mathematically, conditions (4.3) are generic. Namely, there is an open and dense set $U \subset X \times L^2(\Omega,\mathbb{R}^2)$, such that for any $(\varphi, f) \in U$ the solution $u(x,t)$ of (3.1) satisfies (4.3). Hence conditions (4.3) are a physically sound condition. Moreover, in Theorem 4.1, the conditions (4.3) can also be replaced by

$$\frac{\partial u_\tau}{\partial n}(\overline{x},t) \quad \text{or} \quad u_\tau(\overline{x},t) \begin{cases} > 0 & \text{for } t < t_0 \quad (\text{or } t > t_0), \\ = 0 & \text{for } t = t_0, \\ < 0 & \text{for } t > t_0 \quad (\text{or } t < t_0). \end{cases}$$

4.2. **Separation equations for the rigid boundary condition.** To verify the condition (4.1), it is very useful to transform the Navier-Stokes equations (3.1) into the separation equation introduced in this and next subsections.

1). *Separation equation in $(\tau,n)-$representation.* In [5], we proved that the Navier-Stokes equations (3.1) lead to the following boundary-layer separation equation of (3.1) under the rigid boundary condition:

$$\frac{\partial u_\tau(x,t)}{\partial n} = \frac{\partial \varphi_\tau}{\partial n} + \int_0^t [\nu \nabla \times \Delta u + k\nu \Delta u \cdot \tau + \nabla \times f + k f_\tau] \mathrm{d}t, \tag{4.4}$$

where n, τ are the unit normal and tangent vectors on $\partial\Omega$, k is the curvature of $\partial\Omega$ at $x \in \partial\Omega$, and

$$\nabla \times v = \frac{\partial v_\tau}{\partial n} - \frac{\partial v_n}{\partial \tau}. \tag{4.5}$$

2). *Separation equation in $(x_1,x_2)-$representation.* Consider an orthogonal coordinate system (x_1,x_2), the equivalent separation equation of the Navier-Stokes equations was derived in [14]:

$$\frac{\partial u_\tau(x,t)}{\partial n} = -\nabla \times \varphi - \int_0^t [\nu \nabla \times \Delta u + \nabla \times f] \mathrm{d}t, \quad x \in \partial\Omega, \tag{4.6}$$

where $\nabla \times v = \partial v_2/\partial x_1 - \partial v_1/\partial x_2$ for $v = (v_1, v_2)$.

Remark 4.3. Although the curvature k of $\partial\Omega$ doesn't appear in the separation equation (4.6), the curvature of $\partial\Omega$ is hidden in $\nabla \times \Delta u$ and $\nabla \times f$, i.e. in the curl of Δu and f in the orthogonal coordinate system.

4.3. **Separation equation for the free boundary condition.** Consider the Navier-Stokes equations with the free boundary condition:

$$\frac{\partial u}{\partial t} + (u \cdot \nabla)u = \nu \Delta u - \frac{1}{\rho}\nabla p + f, \tag{4.7}$$

$$\mathrm{div} u = 0, \tag{4.8}$$

$$\begin{cases} u_n = 0, \quad \dfrac{\partial u_\tau}{\partial n} = 0 \quad \text{on } \partial\Omega, \\ u(x,0) = \varphi(x). \end{cases} \tag{4.9}$$

To deduce the separation equation of (4.7)–(4.9), we recall that for any external $f \in L^2(\Omega, \mathbb{R}^2)$, as a vector field we know that f can be uniquely decomposed as

$$f = F + \nabla\phi, \quad \mathrm{div} F = 0, \ \text{ and } F_n = 0 \ \text{ on } \partial\Omega. \tag{4.10}$$

Also, $(u \cdot \nabla)u$ is decomposed as

$$\begin{aligned} &(u \cdot \nabla)u = g(u) + \nabla\Phi(u), \\ &\mathrm{div} g(u) = 0, \quad g_n|_{\partial\Omega} = 0. \end{aligned} \tag{4.11}$$

Then in the following we shall prove that the separation equation of (4.7)–(4.9) is written in the following form

$$u_\tau(x,t) = \varphi_\tau(x) + \int_0^t \left[\nu \left(\frac{\partial^2 u_\tau}{\partial \tau^2} + \frac{\partial^2 u_\tau}{\partial n^2} \right) - g_\tau(u) + F_\tau \right] \mathrm{d}t, \tag{4.12}$$

where F and g are as in (4.10) and (4.11).

Remark 4.4. If the portion of the boundary $\Gamma \in \partial\Omega$ is flat:

$$\Gamma = \{(x_1, x_2) \in \partial\Omega \mid -\delta < x_1 < \delta, \ x_2 = 0\}, \tag{4.13}$$

and the velocity gradient $\partial u_1 / \partial x_1$ is small on Γ, then the equation (4.12) can be approximatively written as

$$\begin{aligned} &u_1(x,t) = \varphi_1 + \int_0^t [\nu \Delta u_1 + F_1 - A] \mathrm{d}t, \quad x = (x_1, 0), \\ &A = u_1 \frac{\partial u_1}{\partial x_1}\bigg|_{x=0}, \end{aligned} \tag{4.14}$$

where u_1, φ_1, and F_1 are the x_1-components of u, φ and F. □

We are now in position to verify (4.12). By (4.8) and (4.9), we induce from the free boundary condition that

$$\triangle u \cdot n|_{\partial\Omega} = 0,$$

and consequently

$$\mathrm{div}(\Delta u) = 0.$$

Hence, by (4.10) and (4.11), equation (4.7) can be decomposed as

$$\begin{aligned} &\frac{\partial u}{\partial t} = \nu\Delta u - g(u) + F, \\ &\frac{1}{\rho}p = \phi - \Phi(u). \end{aligned} \tag{4.15}$$

Then, we derive from the first equation of (4.15) that

$$u_\tau = \varphi_\tau + \int_0^t [\nu\Delta u_\tau - g_\tau(u) + F_\tau]\mathrm{d}t,$$

which is the equation (4.12).

We now verify (4.14). By (4.9), it is clear that

$$(u\cdot\nabla)u\cdot\tau = u_1\frac{\partial u_1}{\partial x_1} \quad \text{on } \Gamma. \tag{4.16}$$

By (4.11), in the divergence-free part $g = (g_1, g_2)$ of $(u\cdot\nabla)u$, $g_1|_{x=0}$ represents the leading order of g_1. Hence the Taylor expression of g_1 on Γ is given by

$$g_1(x_1) = g_1(0) + x_1 f(x_1), \quad f_1 = g'(0) + \frac{1}{2}g_1''(0)x_1 + o(x_1).$$

Since $\partial u_1/\partial x_1$ is small on Γ, by (4.11) and (4.16) we have

$$g_1(0) \gg x_1 f(x_1) \text{ for } (x_1, 0) \in \Gamma.$$

Hence, we get that

$$g_1(0) = u_1\frac{\partial u_1}{\partial x_1}\bigg|_{x=0} \simeq g_\tau(x) \ \text{ on } \Gamma.$$

Replacing g_τ in (4.12) by $g_1(0)$, we obtain (4.14).

We note that the separation equation (4.14) is more useful than (4.12) in dealing with fluid boundary-layer separations.

5. Predicable Conditions and Critical Thresholds

5.1. **Predicable condition.** Predicable problem for boundary-layer separations of 2D fluid flows governed by Navier-Stokes equations is an important topic in both classical and geophysical fluid dynamics. It mainly concerns when, where, and how a boundary-layer separation will occur. In particular, we need to know the conditions for the separation to appear in terms of the initial values and the external forces that are observable. Based on the basic theory introduced in the last section, we now address this problem.

1). *Predicable condition of flows with Dirichlet boundary condition on a flate boundary.* When the separation occurs on a flat portion Γ of

$\partial\Omega$, a predicable condition was given in [3]. For the sake of completeness, we introduce it in the following.

Let $\Gamma \subset \partial\Omega$ be as in (4.13), and $x_2 > 0$ be the interior of Ω. By

$$\varphi|_{\partial\Omega} = 0, \qquad \text{div}\varphi = 0,$$

near Γ, the initial value $\varphi = (\varphi_1, \varphi_2)$ can be expressed as

$$\begin{aligned} &\varphi_1 = x_2\varphi_{11}(x_1) + x_2^2\varphi_{12}(x_1) + x_2^3\varphi_{13}(x_1) + o(x_2^3), \\ &\varphi_2 = x_2^2\varphi_{21}(x_1) + o(x_2^3), \\ &\varphi_{21} = -\frac{1}{2}\varphi_{11}'. \end{aligned} \tag{5.1}$$

The first-order Taylor expression of the external force f on x_2 near Γ is given by

$$\begin{aligned} f_1 &= f_{11}(x_1) + x_2 f_{12}(x_1) + o(x_2), \\ f_2 &= f_{21}(x_1) + x_2 f_{22}(x_1) + o(x_2). \end{aligned} \tag{5.2}$$

If the following condition holds true

$$0 < \min_{\Gamma} \frac{-\varphi_{11}}{2\nu\varphi_{11}'' + 6\nu\varphi_{13} + f_{12} - f_{21}'} \ll 1, \tag{5.3}$$

then there are $t_0 > 0$ and $x_0 \in \Gamma$ such that the solution u of (3.1) has a boundary layer separation at (x_0, t_0), where ν is the viscosity, φ_{11}, φ_{13}, f_{12}, f_{21} are as in (5.1) and (5.2). In addition, t_0 and $x_0 = (x_1^0, 0)$ approximately satisfy

$$t_0 = g(x_0), \quad \text{and} \quad g(x_0) = \min_{\Gamma} g(x), \tag{5.4}$$

where

$$g = \frac{-\varphi_{11}}{2\nu\varphi_{11}'' + 6\nu\varphi_{13} + f_{12} - f_{21}'}.$$

The condition (5.3), expressed in terms of the initial value φ and the external force f, provides a criterion for a boundary-layer separation to occur at (x_0, t_0), and the relations in (5.4) give the time t_0 and the position x_0 where the separation occurs.

The proof (5.3) is based on Theorem 4.1 by applying the separation equation (4.4). In fact, on Γ (4.4) can be written as

$$\frac{\partial u_1(x,t)}{\partial x_2} = \frac{\partial \varphi_1}{\partial x_2} + \int_0^t \left[\nu\frac{\partial \Delta u_1}{\partial x_2} - \nu\frac{\partial \Delta u_2}{\partial x_1} + \frac{\partial f_1}{\partial x_2} - \frac{\partial f_2}{\partial x_1}\right] \mathrm{d}t. \tag{5.5}$$

Take the first-order expression of u on t as

$$u = \varphi + tu'(x,t),$$

and insert it in the right side of (5.5). By (5.1) and (5.2), we obtain that

$$\frac{\partial u_1}{\partial x_2} = \varphi_{11} + t[\nu(\varphi_{11}'' + 6\varphi_{13} - 2\varphi_{21}') + f_{12} - f_{21}'] + o(t).$$

Note that $\varphi_{21} = -\frac{1}{2}\varphi_{11}''$. Then we have

$$\frac{\partial u_1}{\partial x_2} = \varphi_{11} + t[\nu(2\varphi_{11}'' + 6\varphi_{13}) + f_{12} - f_{21}'] + o(t). \tag{5.6}$$

Then, under the condition (5.3), we deduce that there are $x_0 \in \Gamma$ and $t_0 > 0$ sufficiently small such that

$$\frac{\partial u_\tau}{\partial n}(t, x_0) \begin{cases} \neq 0 & \text{for } 0 \le t < t_0, \\ = 0 & \text{for } t = t_0. \end{cases}$$

$$\frac{\partial}{\partial t}\frac{\partial u_\tau}{\partial n}\bigg|_{(t_0, x_0)} \neq 0.$$

Conclusions of (5.3) and (5.4) follow then from Theorem 4.1.

2). *Predicable condition for flows with Dirichlet boundary condition on a curved boundary.* On a curved boundary, a predicable condition for boundary-layer separations can be derived from the separation equations (4.4) and (4.6) respectively, also based on Theorem 4.1.

Let $\Gamma \subset \partial\Omega$ be an open and curved portion of the boundary. By (4.4), we can derive the following predicable condition:

$$0 < \min_{\Gamma} \frac{-\frac{\partial \varphi_\tau}{\partial n}}{\nu(\nabla \times \Delta\varphi + k\Delta\varphi \cdot \tau) + \nabla \times f + k f_\tau} \ll 1, \tag{5.7}$$

where $k = k(x)$ is the curvature of $\partial\Omega$ at $x \in \Gamma$, and $\nabla \times v$ is as in (4.5) for the vector field v.

The other predicable condition in the orthogonal coordinate (x_1, x_2) can be derived from (4.6) as follows (see [14]),

$$0 < \min_{\Gamma} \frac{\frac{\partial \varphi_2}{\partial x_1} - \frac{\partial \varphi_1}{\partial x_2}}{\nu\left(\frac{\partial \Delta\varphi_1}{\partial x_2} - \frac{\partial \Delta\varphi_2}{\partial x_1}\right) + \frac{\partial f_1}{\partial x_2} - \frac{\partial f_2}{\partial x_1}} \ll 1. \tag{5.8}$$

3). *Predicable conditions of free boundary condition.* By the separation equations (4.12) and (4.14), based on Theorem 4.1, we can also derive predicable conditions for fluid flows with the free boundary condition.

If $\Gamma \subset \partial\Omega$ is a flat portion of the boundary, as given by (4.13), we have the following criterion to determine a boundary-layer separation

to occur on Γ:

$$0 < \min_{\Gamma} \frac{-\varphi_1}{\nu\Delta\varphi_1 + F_1 - \varphi_1 \frac{\partial\varphi_1}{\partial x_1}\big|_{x=0}} \ll 1, \tag{5.9}$$

where φ_1 and F_1 are the x_1-components of φ and F, and F is as in (4.10). If $\Gamma \subset \partial\Omega$ is curved, then by (4.12) we deduce the following predicable condition:

$$0 < \min_{\Gamma} \frac{-\varphi_\tau}{\nu\left(\frac{\partial^2\varphi_\tau}{\partial\tau^2} + \frac{\partial^2\varphi_\tau}{\partial n^2}\right) + F_\tau - g_\tau(\varphi)} \ll 1, \tag{5.10}$$

where g is as in (4.11).

The five criteria (5.3) and (5.7)–(5.10) for boundary-layer separations are very useful in wide range of applications.

Remark 5.1. With conditions (5.3) and (5.7)–(5.10), the critical time t_0 might appear to be very small; see for example (5.4). However, this misperception is related to scaling. For a large scale fluid motion, the underlying dimensions are large, and the time t_0 is not small in real applications.

5.2. **Critical curvature of boundary tip point.** To discuss vortices separated from a boundary tip point we need to use the separation equation (4.4). Let t_0 be the elapsed time between the instant when a vortex separated from the tip point disappears and the time when a new one forms. The elapsed time t_0 is called the relaxation time for the tip point separation.

Let $x_0 \in \partial\Omega$ be a boundary tip point with curvature k. Take k as the control parameter. Then, equation (4.4) becomes

$$\begin{aligned}\frac{\partial u_\tau(k)}{\partial n} =& \frac{\partial\varphi_\tau(x_0)}{\partial n} + \left(\frac{\partial f_\tau(x_0)}{\partial n} - \frac{\partial f_n(x_0)}{\partial\tau} + k f_\tau(x_0)\right) t_0 \\ &+ \int_0^{t_0} \nu\left[\frac{\partial(\Delta u\cdot\tau)}{\partial n} - \frac{\partial(\Delta u\cdot n)}{\partial\tau} + k\Delta u\cdot\tau\right]_{x_0} \mathrm{d}t.\end{aligned} \tag{5.11}$$

Here, the initial injection flow $\varphi(x)$ is taken parallel to the tangent vector τ at x_0, i.e. φ represents a parallel gradient flow as

$$\varphi = (ax_2, 0) \quad \text{near} \quad x_0 \in \partial\Omega, \tag{5.12}$$

where the coordinate (x_1, x_2) is taken so that the x_1-axis is in the tangent $\tau-$direction, x_2-axis is in the normal $n-$direction, and x_0 is the origin of this coordinate system; see Figure 5.1. By the definition of the relaxation time, it is known that t_0 is very small. Hence we have

$$u(x,t) \simeq \varphi \quad \forall\ 0 \le t < t_0 \quad \text{near } x_0 \in \partial\Omega.$$

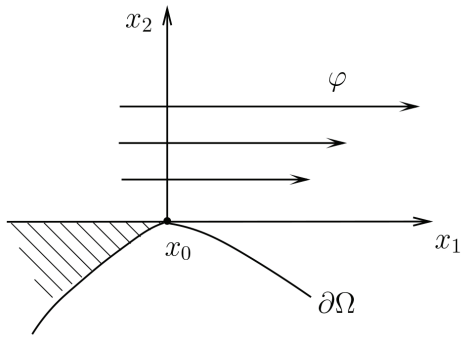

FIGURE 5.1. A schematic diagram of parallel gradient flow near a boundary tip point x_0, the shadow part is a dead angle where fluid velocity $u = 0$.

By (5.12), this implies that

$$\int_0^{t_0} \left[\frac{\partial(\Delta u \cdot \tau)}{\partial n} - \frac{\partial(\Delta u \cdot n)}{\partial \tau} + k\Delta u \cdot \tau \right]_{x_0} \mathrm{d}t \simeq 0,$$

and (5.11) can be approximatively written as

$$\frac{\partial u_\tau(k)}{\partial n} = a + k f_\tau t_0 + \left(\frac{\partial f_\tau}{\partial n} - \frac{\partial f_n}{\partial \tau} \right) t_0. \tag{5.13}$$

Because f is the resistance force generated by the friction at x_0, it is reversely parallel to φ, and we have

$$\frac{\partial f_n}{\partial \tau} = 0, \qquad \frac{\partial f_\tau}{\partial n} \simeq 0.$$

Thus, (5.13) becomes

$$\frac{\partial u_\tau(k)}{\partial n} = a + k f_\tau t_0 \quad (a > 0,\ f_\tau < 0). \tag{5.14}$$

For the control parameter k (instead of t), it follows from (5.14) that

$$\begin{aligned} &\frac{\partial u_\tau(k)}{\partial n} \begin{cases} < 0 & \text{for } k < k_c, \\ = 0 & \text{for } k = k_c, \end{cases} \\ &\frac{\partial}{\partial k} \frac{\partial u_\tau(k_c)}{\partial n} = f_\tau t_0 \neq 0, \end{aligned} \tag{5.15}$$

where k_c is the critical curvature, given by

$$k_c = \frac{a}{|f_\tau| t_0}. \tag{5.16}$$

Namely, by the boundary-layer separation theorem, Theorem 4.1, under the conditions (5.15), the critical curvature k_c in (5.16) is the critical threshold where vortices begin to form.

Physically, $a = |\nabla\varphi(x_0)|$ is the strength of the injection velocity, which is proportional to the viscosity ν:

$$a = \gamma\nu \qquad (\gamma \text{ is the coefficient}).$$

The frictional force f_τ is proportional to the smoothness of the material surface, denoted by κ:

$$f_\tau = \theta\kappa,$$

where θ is the proportional coefficient. Therefore, the critical curvature k_c in (5.16) is

$$k_c = \frac{\alpha\nu}{\kappa t_0}, \tag{5.17}$$

where $\alpha = \gamma/\theta$ is the proportional coefficient.

Formula (5.17) shows that the vortices are easier to form if the viscosity of fluid is relatively small, and the surface of the material is rougher (i.e. κ is relatively large). This conforms to the physical reality.

5.3. **Critical velocity of surface turbulence.** For a boundary flow, when the injection velocity u_0 is smaller than a critical threshold u_c, it is a parallel shear flow, and when $u_0 > u_c$, surface turbulence occurs. The threshold u_c is defined as

$$u_c = \text{the critical velocity of boundary-layer separation.} \tag{5.18}$$

Based on this definition, to obtain the critical threshold u_c of surface turbulence, we only need to consider the critical injection velocity u_0 at which the boundary-layer separation occurs. We use the separation equation (4.14) for the free boundary condition to study this problem.

Let $t_0 > 0$ be the relaxation time when the first vortex appears as the injection velocity u_0 arrives at u_c, so that $t_0 > 0$ is small. Hence, (4.14) can be approximatively written in the form

$$u_\tau = \varphi_\tau + \left[F_\tau + \nu\left(\frac{\partial^2\varphi_\tau}{\partial\tau^2} + \frac{\partial^2\varphi_\tau}{\partial n^2}\right) - \varphi_\tau\frac{\partial\varphi_\tau}{\partial\tau}\bigg|_{x=0}\right]t_0, \tag{5.19}$$

where F_τ represents the tangent damping resistance, and $\Gamma \subset \partial\Omega$ is

$$\Gamma = \{(x_1, 0) \mid 0 < x_1 < L\}. \tag{5.20}$$

Let u_0 be the injection velocity. Take u_0 as the control parameter, and

$$\varphi_\tau = u_0 - \beta_1 x_1 + \beta_2 x_1^2 \qquad (\beta_1 > \beta_2 L), \tag{5.21}$$

where $\beta_1,\ \beta_2 > 0$ are two small parameters, depending on the viscosity ν of the fluid and the surface physical property of Γ. By the physical law of the damping force,

$$F_\tau = -\gamma u_0^k \quad (k > 1,\ \gamma > 0). \tag{5.22}$$

Inserting (5.21) and (5.22), we deduce that

$$u_\tau = u_0 - \beta_1 x_1 + \beta_2 x_1^2 - (\gamma u_0^k - 2\beta_2\nu - \beta_1 u_0)t_0.$$

Because $\beta_1 x_1$ and $\beta_2 x_1^2$ are relatively small with respect to u_0, and ν is very small, u_τ can be expressed as

$$u_\tau = (1 + \beta_1 t_0)u_0 - \gamma u_0^k t_0.$$

Let $u_\tau = 0$. Then we obtain the following form of u_c:

$$u_c = \left(\frac{1}{\gamma t_0} + \frac{\beta_1}{\gamma}\right)^{1/(k-1)} \qquad (k > 1), \tag{5.23}$$

where γ is the damping coefficient, depending on the surface property of Γ, and β_1 is as in (5.21) which is an increasing function of the viscosity ν. Let $\beta_1 = \beta_0\nu$. Then (5.23) is rewritten as

$$u_c = \left[\frac{1}{\gamma}\left(\frac{1}{t_0} + \beta_0\nu\right)\right]^{1/(k-1)}. \tag{5.24}$$

Remark 5.2. For the surface turbulent problem, the length L in (5.20) cannot be too large because the velocity decay formula (5.21) holds true only for L not large. In fact, the physical phenomena show that surface fluid turbulence can occur only for L being relative small.

6. Boundary-Layer Separation of Ocean Circulations

The atmospheric and oceanic flows exhibit recurrent large-scale patterns. The formation of these patterns are important topological phase transition problem. The main objective of this section is to study the mechanism for the formation of the subpolar gyre and the vortices separated from the western boundary of the Atlantic ocean.

6.1. **Vortices separated from the boundary.**

Let $\Gamma \subset \partial\Omega$ be a flat portion of the coast, denoted by

$$\Gamma = \{(x_1, 0) \mid -\delta < x_1 < \delta\} \tag{6.1}$$

and $x_2 > 0$ represents the sea area. Let $\varphi = (\varphi_1, \varphi_2)$ represent the oceanic flow, expressed as

$$\varphi_1 = \frac{x_2 u_0}{2\delta + x_1}, \qquad \varphi_2 = \frac{x_2^2 u_0}{2(2\delta + x_1)^2} \tag{6.2}$$

where δ is as in (6.1), satisfying

$$\delta \gg 1, \quad u_0 = o(1). \tag{6.3}$$

Consider the wind-driven force $f = (f_1, f_2)$ as

$$f_1 = f_1(x_1), \qquad f_2 = -\frac{1}{2}x_1^2 + 2\delta x_1 + 5\delta^2. \tag{6.4}$$

In view of (5.1) and (5.2), for (6.2) and (6.4) we see that

$$\varphi_{11} = \frac{u_0}{2\delta + x_1}, \qquad \varphi_{13} = 0,$$
$$f_{12} = 0, \qquad f_{12} = -\frac{1}{2}x_1^2 + 2\delta x_1 + 5\delta^2,$$

and the function

$$g(x_1) = \frac{-\varphi_{11}}{2\nu\varphi_{11}'' + 6\nu\varphi_{13} + f_{12} - f_{21}'} = \frac{(2\delta + x_1)^2 u_0}{(2\delta + x_1)^3(2\delta - x_1) - 2\nu u_0}.$$

By (6.3) we have

$$0 < g(x_1) \ll 1 \qquad \forall \ -\delta < x_1 < \delta.$$

It follows from (5.3) that under the wind-driven action of (6.4), the oceanic flow represented by (6.2) will generate a vortex from the boundary Γ. In addition, by (6.3) and $0 < \nu \ll 1$,

$$\min_{\Gamma} g(x_1) \simeq \frac{u_0}{(2\delta + x_1)(2\delta - x_1)}\bigg|_{x_1=0} = \frac{u_0}{4\delta^2}.$$

Then we derive from (5.4) that the separation position x_1° and the time t_0 are given by

$$x_1^\circ = 0, \qquad t_0 = \frac{u_0}{4\delta^2}.$$

Figure 6.1 schematically show the oceanic flow diagram of the wind-driven force (6.4)

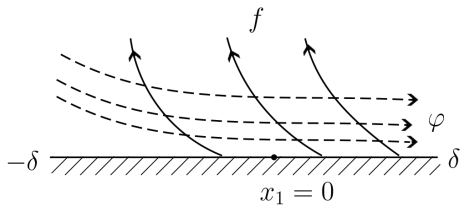

FIGURE 6.1. Solid lines represent the wind, and the dashed lines stand for the oceanic flow.

6.2. **Wind-driven north Atlantic gyres.** In Section 3.1 we introduced the north Atlantic gyres, where a double gyres (as shown in Figure 3.5(a)) is permanent, and some small vortices (as shown in Figure 3.5(b)) is seasonal. In this section we discuss the wind-driven vortices by applying the boundary-layer separation theory.

The dynamical equations governing the wind-driven north Atlantic circulations are the Navier-Stokes equations with free boundary condition, given by

$$\begin{aligned}
&\frac{\partial u}{\partial t} + (u\cdot\nabla)u = \nu\Delta u - \beta y\vec{k}\times u - \frac{1}{\rho}\nabla p + f, \quad (x,y)\in\Omega,\\
&\mathrm{div} u = 0,\\
&u_n|_{\partial\Omega} = 0,\ \left.\frac{\partial u_\tau}{\partial n}\right|_{\partial\Omega} = 0,\\
&u(0) = \varphi,
\end{aligned} \tag{6.5}$$

where the domain Ω represents the north Atlantic region, approximatively in a rectangular region, as

$$\Omega = (0, L)\times(-L, L),$$

with coordinate (x, y), and the $x-$axis points eastward, the $y-$axis is northward, $y = 0$ represents the mid-latitude. The term representing the Coriolis force in (6.5) is

$$-\beta y\vec{k}\times u = -\beta y(-u_2, u_1),$$

where βy is the first-order approximation parameter of the Coriolis force. The wind-driven force f can be expressed as

$$f = F + \mathcal{F}, \tag{6.6}$$

where F is the constant force driving the permanent double gyre as shown in Figure 3.5 (a), and $\mathcal{F}$ represents the force by seasonal winds. For convenience, $\mathcal{F}$ is written in the divergence free part, by (4.12) and (4.14), which dictates the boundary-layer separation:

$$\mathcal{F} = \lambda(\mathcal{F}_1, \mathcal{F}_2), \text{ with } \mathcal{F}_2(0, y) > 0 \text{ for } y < L, \tag{6.7}$$

where λ is the strength, $\mathrm{div}\mathcal{F} = 0$, and $\mathcal{F}\cdot n|_{\partial\Omega} = 0$.

The initial field φ represents the north Atlantic double gyre, which satisfies the stationary equation of (6.5):

$$\begin{aligned}
&\nu\Delta\varphi - \beta y\vec{k}\times\varphi - (\varphi\cdot\nabla)\varphi - \frac{1}{\rho}\nabla p + F = 0,\\
&\mathrm{div}\varphi = 0,
\end{aligned} \tag{6.8}$$

with the free boundary condition, where F is as in (6.6).

To use the separation equation (4.14), we take

$$\Gamma = \{(0, y) \in \partial\Omega \mid 0 < y < L\}.$$

Since $u_n|_{\partial\Omega} = 0$, we have

$$(\vec{k} \times u) \cdot \tau|_{\partial\Omega} = 0.$$

Hence, in view of (6.5)–(6.8), the equation (4.14) can be written as

$$u_2(y,t) = \varphi_2(y) + \int_0^t \left[\nu\Delta u_2 - u_2 \frac{\partial u_2}{\partial y}\bigg|_{y=0} + f_2\right] \mathrm{d}t. \tag{6.9}$$

Let u be denoted by

$$u = \varphi + v \quad \text{with} \quad v|_{t=0} = 0. \tag{6.10}$$

Putting u_2 of (6.10) in the right-side of (6.9), by (6.6)–(6.8), we obtain that

$$u_2(y,t) = \varphi_2(y) + \int_0^t \left[\nu\Delta u_2 - \varphi_2 \frac{\partial v_2}{\partial y} - v_2 \frac{\partial \varphi_2}{\partial y} - \lambda\mathcal{F}_2\right] \mathrm{d}t. \tag{6.11}$$

for $0 < y < L$.

Fixing $t_0 > 0$ small, then by $v(y, 0) = 0$ and (6.7), the equation (6.11) can be approximatively expressed in the form

$$u_2(y, t_0) = \varphi_2(y) + \lambda t_0 \mathcal{F}_2(y). \tag{6.12}$$

By (6.8), in the region of $0 < y < L$, the field φ describes the north Atlantic subpolar gyre, i.e. the northern counter-clockwise gyre in Figure 3.5(a). Hence, we have

$$\begin{aligned} &\varphi_2(y) < 0 \qquad \text{for } 0 < y < L, \\ &\varphi_2(0) = \varphi_2(L) = 0. \end{aligned} \tag{6.13}$$

In addition, by (6.7) and $\mathcal{F} \cdot n|_{\partial\Omega} = 0$, for the rectangular Ω we have

$$\begin{aligned} &\mathcal{F}_2(y) > 0, \quad \text{for } 0 < y < L, \\ &\mathcal{F}_2(L) = 0. \end{aligned} \tag{6.14}$$

It is clear that $\varphi_2 \neq \mathcal{F}_2$. Hence it follows from (6.12)–(6.14) that there are $\lambda_c > 0$ and an isolated point $y_0 \in (0, L)$ such athat

$$u_2(y_0, \lambda) \begin{cases} < 0 & \text{for } \lambda < \lambda_c, \\ = 0 & \text{for } \lambda = \lambda_c, \\ > 0 & \text{for } \lambda > \lambda_c. \end{cases} \tag{6.15}$$

By Theorem 4.1 or Remark 4.2, we infer from (6.15) that the solution u of (6.1) has a boundary-layer separation at $(0, y_0) \in \Gamma$ for $\lambda > \lambda_c$. Namely, we have proved the following physical conclusion.

Physical Conclusion 6.1. *If the mid-latitude seasonal wind strength λ exceeds certain threshold λ_c, vortices near the north Atlantic coast will form, as shown in Figure 3.5(b). Moreover, the scale (radius) of the vortices is an increasing function of $\lambda - \lambda_c$.*

6.3. **North Atlantic subpolar gyre.** The North Atlantic double gyres are formed by the northern subpolar gyre and the southern subtropical gyre. The subtropical gyre is caused mainly by winds, and the subpolar gyre is generated by the Gulf stream along the western boundary and the regional topography; see Figure 6.2 in which a schematically topographic diagram of the North Atlantic double gyre is illustrated. Here we shall discuss the mathematical mechanism for

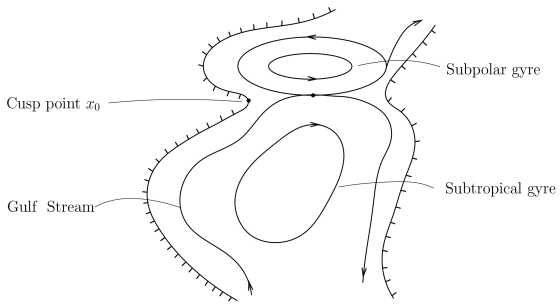

FIGURE 6.2. A schematically topography diagram of the North Atlantic double gyre: the northern subpolar and the southern subtropical gyre.

the subpolar gyre formation by applying the separation equation (4.4); we shall see that the topographical influence of the North Atlantic, i.e. the curvature $k(x_0)$ of the tip point x_0 in Figure 6.2, plays a very important role for the formation of the subpolar gyre.

In a neighborhood of the point x_0, we take the coordinate (x_1, x_2) with x_0 as its origin, the x_1-axis in the tangent direction pointing southward, and the x_2-axis in the normal direction pointing eastward; see Figure 6.3. Take $t_0 > 0$ small, then the separation equation (4.4) at x_0 (i.e. $x = 0$) can be approximatively written as

$$\begin{aligned}\frac{\partial u_\tau(k)}{\partial n} =& \frac{\partial \varphi_\tau(x_0)}{\partial n} + \nu t_0 \left[\frac{\partial(\Delta\varphi \cdot \tau)}{\partial n} - \frac{\partial(\Delta\varphi \cdot n)}{\partial \tau} + k\Delta\varphi \cdot \tau \right]_{x_0} \\ &+ \left(\frac{\partial f_\tau(x_0)}{\partial n} - \frac{\partial f_n(x_0)}{\partial \tau} + k f_\tau(x_0) \right) t_0,\end{aligned} \tag{6.16}$$

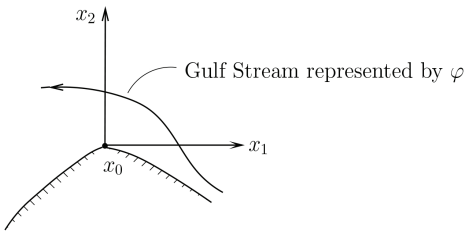

FIGURE 6.3

where k is the curvature of $\partial\Omega$ at x_0 ($x = 0$). Because φ represents the Gulf stream, and $\varphi|_{\partial\Omega} = 0$, we have

$$\frac{\partial\varphi_\tau(0)}{\partial n} = \frac{\partial\varphi_1(0)}{\partial x_2} < 0 \quad \text{(see Figure 6.2)},$$
$$\Delta\varphi\cdot\tau|_{x=0} = \frac{\partial^2\varphi_1(0)}{\partial x_2^2},$$

Due to the curvature $k \gg 1$, if

$$\frac{\partial^2\varphi_1(0)}{\partial x_2^2} \neq 0, \qquad f_1(0) \neq 0,$$

then we can ignore the following terms in (6.16)

$$\nu t_0\left(\frac{\partial(\Delta\varphi\cdot\tau)}{\partial n} - \frac{\partial(\Delta\varphi\cdot n)}{\partial\tau}\right) \quad \text{and} \quad \frac{\partial f_\tau}{\partial n} - \frac{\partial f_n}{\partial\tau}.$$

Then (6.16) becomes

$$\frac{\partial u_\tau(k)}{\partial n} = -\left|\frac{\partial\varphi_1(0)}{\partial x_2}\right| + kt_0\left[f_1(0) + \nu\frac{\partial^2\varphi_1(0)}{\partial x_2^2}\right]. \tag{6.17}$$

Under the following condition

$$f_1(x_0) + \nu\frac{\partial^2\varphi_1(0)}{\partial x_2^2} > 0, \tag{6.18}$$

by (6.17) we deduce that there is a $k_c > 0$ such that

$$\frac{\partial u_\tau(k)}{\partial n}\begin{cases} < 0 & \text{for } k < k_c, \\ = 0 & \text{for } k = k_c, \\ > 0 & \text{for } k > k_c. \end{cases} \tag{6.19}$$

By Theorem 4.1, it follows from (6.19) that if $k > k_c$, then there exists a counter-clockwise gyre in the north of the subtropic gyre. Hence, we have the following results.

Physical Conclusion 6.2. *The condition for the subpolar gyre to appear is that the curvature k of $\partial\Omega$ at x_0 in Figure 6.2 is sufficiently large, and the Gulf stream velocity field $\varphi = (\varphi_1, \varphi_2)$ and external forcing $f = (f_1, f_2)$ at x_0 satisfy the inequality* (6.18).

References

[1] M. Ghil, T. Ma, and S. Wang, *Structural bifurcation of 2-D incompressible flows*, Indiana Univ. Math. J., 50 (2001), pp. 159–180. Dedicated to Professors Ciprian Foias and Roger Temam (Bloomington, IN, 2000).

[2] J. M. Kosterlitz and D. J. Thouless, *Ordering, metastability and phase transitions in two-dimensional systems*, Journal of Physics C: Solid State Physics, 6 (1973), p. 1181.

[3] H. Luo, Q. Wang, and T. Ma, *A predictable condition for boundary layer separation of 2-d incompressible fluid flows*, Nonlinear Anal. Real World Appl., 22 (2015), pp. 336–341.

[4] T. Ma and S. Wang, *Boundary layer separation and structural bifurcation for 2-D incompressible fluid flows*, Discrete Contin. Dyn. Syst., 10 (2004), pp. 459–472. Partial differential equations and applications.

[5] ——, *Geometric theory of incompressible flows with applications to fluid dynamics*, vol. 119 of Mathematical Surveys and Monographs, American Mathematical Society, Providence, RI, 2005.

[6] ——, *Boundary-layer and interior separations in the Taylor-Couette-Poiseuille flow*, J. Math. Phys., 50 (2009), pp. 033101, 29.

[7] ——, *Phase Transition Dynamics*, Springer-Verlag, xxii, 555pp., 2013.

[8] ——, *Topological Phase Transition V: Interior Separation and Cyclone Formation Theory*, in preparation, (2017).

[9] ——, *Topological Phase Transitions I: Quantum Phase Transitions*, Hal preprint: `hal-01651908`, (2017).

[10] ——, *Topological Phase Transitions II: Spiral Structure of Galaxies*, Hal preprint: `hal-01671178`, (2017).

[11] ——, *Topological Phase Transitions III: Solar Surface Eruptions and Sunspots*, Hal preprint: `hal-01672381`, (2017).

[12] H. Oertel, *Prandtl-Führer durch die Strömungslehre*, Vieweg+Teubner Verlag, 2001.

[13] L. Prandtl, in Verhandlungen des dritten internationalen Mathematiker-Kongresses, Heidelberg, Leipeizig, pp. 484-491, 1904.

[14] Q. Wang, H. Luo, and T. Ma, *Boundary layer separation of 2-d incompressible dirichlet flows*, Discrete Contin. Dyn. Syst. Ser. B, 20 (2015), pp. 675–682.

(Ma) Department of Mathematics, Sichuan University, Chengdu, P. R. China

E-mail address: `matian56@sina.com`

(Wang) Department of Mathematics, Indiana University, Bloomington, IN 47405

E-mail address: `showang@indiana.edu`